ISBN: 978-3-95450-236-3 ISSN: 2673-5350 doi:10.18429/JACoW-IBIC2023-WEP034

EFFECT OF LONGITUDINAL BEAM-COUPLING IMPEDANCE ON THE SCHOTTKY SPECTRUM OF BUNCHED BEAMS

C. Lannoy[1,*], D. Alves, K. Lasocha, N. Mounet, CERN, Geneva, Switzerland
T. Pieloni, EPFL, Lausanne, Switzerland
[1]also at EPFL, Lausanne, Switzerland

Abstract

Schottky spectra can be strongly affected by collective effects, in particular those arising from beam-coupling impedance when a large number of bunch charges are involved. In such conditions, the direct interpretation of the measured spectra becomes difficult, which prevents the extraction of beam and machine parameters in the same way as is usually done for lower bunch charges. Since no theory is yet directly applicable to predict the impact of impedance on such spectra, we use here time-domain, macro-particle simulations and apply a semi-analytical method to compute the Schottky spectrum for various machine and beam conditions, such as the ones found at the Large Hadron Collider. A simple longitudinal resonator-like impedance model is introduced in the simulations and its effect studied in different configurations, allowing preliminary interpretations of the impact of longitudinal impedance on Schottky spectra.

INTRODUCTION

Theoretical reconstructions of Schottky spectra, such as the matrix formalism proposed in [1, 2], or the Monte Carlo approach used in [3, 4], are based on the assumption that the synchrotron frequency distribution is known. Under certain conditions, one can derive an analytical relation between the amplitude of the synchrotron oscillation and its frequency (see below) allowing these methods to reconstruct the Schottky spectrum from the synchrotron amplitude distribution. However, this relation has to be modified when external forces, such as the one coming from beam-coupling impedance, affect the longitudinal dynamics.

This study will briefly present the available theory relating the amplitude of the synchrotron oscillation to its frequency, as well as a commonly adopted approximation. The second section will deal with the additional external forces coming from impedance, extending the theory presented in [5] to the case of a non-linear radio frequency (RF) bucket. Finally, we will apply the developed theory to the particular case of a longitudinal broad-band resonator, and will benchmark it against macro-particle simulations performed with PyHEADTAIL [4, 6, 7], in the case of a proton bunch in the Large Hadron Collider (LHC).

Synchrotron Oscillation

For an impedance-free environment, the equation of motion for the RF phase ϕ [1] of a given particle is [8, Eq. (9.51)]:

$$\frac{d^2\phi}{dt^2} + \Omega_0^2 \sin\phi = 0, \tag{1}$$

assuming that the synchronous phase ϕ_s is such that $\sin\phi_s$ is small enough to be neglected (i.e. no acceleration or energy loss compensation). The nominal synchrotron frequency[2] reads

$$\Omega_0^2 = \omega_0^2 \frac{-\eta h e \widehat{V}}{2\pi E_0 \beta^2} \cos\phi_s, \tag{2}$$

where e is the elementary charge, and where the relevant machine parameters are: the revolution frequency ω_0, the slippage factor η, the amplitude of the RF voltage $\widehat{V}$, the rf harmonic number h, the relativistic factor β, and the reference energy E_0. Note that by convention η is positive above transition, such that η and $\cos\phi_s$ always have opposite sign.

Equation (1) is similar to the non-linear pendulum equation, hence the synchrotron frequency Ω_s of the particle can be written [9]

$$\Omega_s(\widehat{\phi}) = \frac{\pi}{2\mathcal{K}\left[\sin\left(\frac{\widehat{\phi}}{2}\right)\right]}\Omega_0, \tag{3}$$

where $\widehat{\phi}$ is the RF phase amplitude of the synchrotron oscillation and $\mathcal{K}$ is the complete elliptic integral of the first kind [10, Eq. (8.112.1)].

Equation (1) can also be approximated by replacing the sine function with its Maclaurin series expansion up to the third order, which yields

$$\frac{d^2\phi}{dt^2} + \Omega_0^2 \left(\phi - \frac{\phi^3}{6}\right) + \mathcal{O}(\phi^5) = 0. \tag{4}$$

This last equation has been studied in [9], and an approximation of the oscillation frequency is given by

$$\Omega_s(\widehat{\phi}) = \Omega_0 \left(1 - \frac{\widehat{\phi}^2}{16}\right). \tag{5}$$

Figure 1 illustrates how the exact solution from Eq. (3) compares with the approximation from Eq. (5). The amplitude distribution corresponding to a Gaussian bunch profile of standard deviation $\sigma = 31$ ns is also shown in order to compare the most populated region with the zone where the

[1] Above transition ϕ has to be taken as the difference between the RF phase of the particle and π.
[2] By nominal synchrotron frequency, we mean the limit of the synchrotron frequency for synchrotron amplitudes approaching zero.

* christophe.lannoy@cern.ch

ISBN: 978-3-95450-236-3 ISSN: 2673-5350 doi:10.18429/JACoW-IBIC2023-WEP034

approximation is valid. As can be seen, the approximation holds for an amplitude $\widehat{\phi} \lesssim 0.8\pi$, which is the region where the vast majority of the particles are. Noting that $\phi = h\omega_0\tau$,

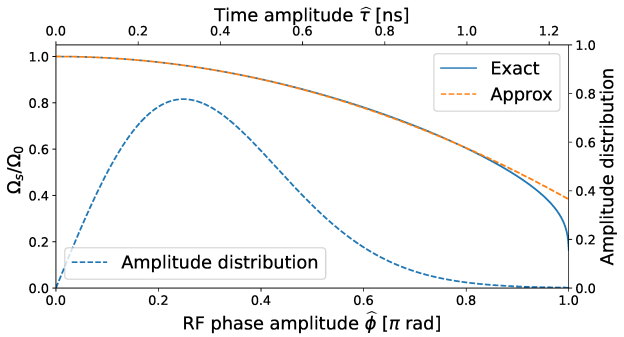

Figure 1: Comparison between the exact and approximate expressions of the synchrotron frequency as a function of the oscillation amplitude. The distribution of amplitudes for a Gaussian bunch is also shown.

with τ the arrival time difference between a given particle and the synchronous particle, we can also express the amplitude of the synchrotron oscillation in terms of the time amplitude defined by

$$\widehat{\tau} \equiv \widehat{\phi}/h\omega_0. \tag{6}$$

THEORETICAL DESCRIPTION

In this section, we investigate the influence of impedance on the longitudinal dynamics of a particle and, more specifically, how it can affect its oscillation frequency. A given force F_i acting longitudinally on the particle will impact the phase dynamics with

$$F_i = \frac{dp}{dt} = \frac{d(p_0+\delta p)}{dt} = \frac{d(\delta p)}{dt} = \frac{p_0}{\eta}\ddot{\tau} = \frac{p_0}{\eta h\omega_0}\ddot{\phi}, \tag{7}$$

where we used the fact that p_0 is constant, the definition of the slippage factor, and Eq. (6). The equation of motion with an additional external force is given by combining Eqs. (1) and (7), which yields

$$\ddot{\phi} + \Omega_0^2 \sin\phi = \frac{\eta h\omega_0}{p_0} F_i(t). \tag{8}$$

Impedance Force

In this study, we will focus on the force arising from the longitudinal beam-coupling impedance, which is given by [11, Eq. (4.18)]

$$\begin{aligned} F_{Imp}(t) &= e\left[\vec{E} + \vec{\beta}c \times \vec{B}\right]_{\parallel}\left(t, z = \beta c\tau(t)\right) \\ &= -\frac{Ne^2}{2\pi C}\int_{-\infty}^{\infty} Z_{\parallel}(\omega)\widehat{\Lambda}(\omega)e^{j\frac{\omega z}{\beta c}}d\omega, \end{aligned} \tag{9}$$

where C stands for the circumference of the accelerator, N for the number of particles in the bunch, $Z_{\parallel}(\omega)$ for the longitudinal impedance, and $\widehat{\Lambda}(\omega)$ for the beam spectrum normalised by the bunch intensity. The force has to be taken at the current position of the particle, i.e. at a distance $z = \beta c\tau$ behind the synchronous particle. Note that the bunch spectrum $\widehat{\lambda}(\omega)$ of [11, Eq. (4.18)], has been replaced by the beam spectrum $\widehat{\Lambda}(\omega)$ in order to take into account the possible multi-turn wake (this approach is equivalent to adding the forces coming from different turns).

The beam spectrum is the Fourier transform of the beam profile. For a single bunch in a circular accelerator, the latter can be expressed as the convolution of the bunch profile $\lambda(t)$ with a Dirac comb of the revolution period T_0. Using the convolution theorem, the beam spectrum can be written

$$\begin{aligned} \widehat{\Lambda}(\omega) &= \mathscr{F}\{\lambda(t) * \text{Ш}_{T_0}(t)\} \\ &= \mathscr{F}\{\lambda(t)\}\,\mathscr{F}\{\text{Ш}_{T_0}(t)\} \\ &= \widehat{\lambda}(\omega)\omega_0\text{Ш}_{\omega_0}(\omega), \end{aligned} \tag{10}$$

where $*$ stands for the convolution operation and where the Dirac comb of period T_0 is defined as follows

$$\text{Ш}_{T_0}(t) = \sum_{p=-\infty}^{\infty}\delta(t - pT_0).$$

Substituting Eq. (10) in Eq. (9) , we have

$$\begin{aligned} F_{Imp}(t) &= \frac{-Ie}{C}\sum_{p=-\infty}^{\infty}\int_{-\infty}^{\infty} Z_{\parallel}(\omega)\widehat{\lambda}(\omega)e^{j\frac{\omega z}{\beta c}}\delta(\omega - p\omega_0)d\omega \\ &= \frac{-Ie}{C}\sum_{p=-\infty}^{\infty} Z_{\parallel}(p)\widehat{\lambda}(p)e^{jp\omega_0\tau(t)}, \end{aligned} \tag{11}$$

where we used the compact notation $Z_{\parallel}(p) \equiv Z_{\parallel}(p\omega_0)$, $\widehat{\lambda}(p) \equiv \widehat{\lambda}(p\omega_0)$, and the average current $I \equiv Ne\frac{\omega_0}{2\pi}$.

General Equation of Motion

Combining Eqs. (2), (6), (8), and (11) yields

$$\ddot{\phi} + \Omega_0^2 \sin\phi = \Omega_0^2\frac{I}{\widehat{V}\cos\phi_s}\sum_{p=-\infty}^{\infty} Z_{\parallel}(p)\widehat{\lambda}(p)e^{j\frac{p}{h}\phi}. \tag{12}$$

By expanding the sine and exponential functions into their Maclaurin series

$$\sin\phi = \sum_{n=0}^{\infty}\frac{(-1)^n}{(2n+1)!}\phi^{2n+1}, \quad e^{j\frac{p}{h}\phi} = \sum_{n=0}^{\infty}\frac{1}{n!}\left(\frac{jp}{h}\right)^n\phi^n,$$

Eq. (12) can be written in the compact form

$$\ddot{\phi} + \Omega_0^2\sum_{n=0}^{\infty} S_n\phi^n = 0, \tag{13}$$

with the coefficients S_n defined by

$$S_n = \begin{cases} -Z_n & : n \text{ even}, \\ \frac{j^{n-1}}{n!} - Z_n & : n \text{ odd}, \end{cases} \tag{14}$$

and

$$\begin{aligned} Z_n &= \frac{I}{\widehat{V}\cos\phi_s}\sum_{p=-\infty}^{\infty} Z_{\parallel}(p)\widehat{\lambda}(p)\frac{1}{n!}\left(\frac{jp}{h}\right)^n \\ &= \frac{Ij^n}{\widehat{V}\cos\phi_s\, n!h^n}\sum_{p=-\infty}^{\infty}\widehat{\lambda}(p)p^n \times \begin{cases} Re[Z_{\parallel}(p)] & : n \text{ even}, \\ j\,Im[Z_{\parallel}(p)] & : n \text{ odd}. \end{cases} \end{aligned}$$

ISBN: 978-3-95450-236-3 ISSN: 2673-5350 doi:10.18429/JACoW-IBIC2023-WEP034

In the last equality, we used the fact that $\widehat{\lambda}(p)$, $Re\left[Z_\parallel(p)\right]$, and $Im\left[Z_\parallel(p)\right]$ are respectively even, even, and odd functions.

The idea behind the expansion performed above is that, for small oscillation amplitudes, only the first order terms can be kept. The shift of the nominal synchrotron frequency is given by S_1 while the non-linear terms will be responsible for an amplitude dependent synchrotron frequency shift.

Broad-Band Resonator

We will now apply Eq. (13) to the particular case of a broad-band resonator described by the following function

$$Z_\parallel^{BB}(\omega) = \frac{R_\parallel}{1 - jQ\left(\frac{\omega_r}{\omega} - \frac{\omega}{\omega_r}\right)},$$

where $R_\parallel$ is the shunt impedance, ω_r the angular cut-off frequency, and Q the quality factor. The values we will use for these parameters are shown in Table 1 and correspond to a first estimate of the broad-band part of the LHC impedance [12, p. 71].

The even terms in Eq. (13) are responsible for the synchronous phase shift and we assume that, in the particular case of a broad-band resonator, their contribution can be neglected. Expanding Eq. (13) up to the third order gives

$$\ddot{\phi} + \Omega_0^2\,(S_1\phi + S_3\phi^3) + \mathcal{O}(\phi^5) = 0, \qquad (15)$$

which is similar to Eq. (4) where the factors 1 and $-\frac{1}{6}$ have been generalised to the arbitrary coefficients S_1 and S_3. In this case, the approximate synchrotron frequency is given by

$$\Omega_s(\widehat{\phi}) = \Omega_0\sqrt{S_1}\left(1 + \frac{3S_3}{8S_1}\widehat{\phi}^2\right), \qquad (16)$$

as can be seen by substituting the function $\phi(t) = \sqrt{A}\Phi(t)$ (with A an arbitrary number) in Eq. (4) and identifying the coefficients.

SIMULATION

The simulation aims at reproducing the typical conditions of an LHC proton fill at injection. The method used to reconstruct the Schottky spectrum from the macro-particle simulation is presented in [4] and the simulation parameters are summarised in Table 1.

Table 1: PyHEADTAIL Simulation Parameters

Intensity	1.5×10^{11} protons per bunch
Energy per proton	450 GeV
Slippage factor	3.436×10^{-4}
RF harmonic	35640
RF voltage	4 MV
LHC circumference	26.659 km
Bunch length (RMS)	$\sigma = 0.31$ ns
Broad-band resonator	
Shunt impedance	$R_\parallel = 31.1\,\mathrm{k}\Omega$
Cut-off frequency	$\omega_r = 2\pi \times 5$ GHz
Quality factor	$Q = 1$

Figure 2 presents an overall view (upper plot) of the simulated longitudinal Schottky spectrum together with a detailed view of two regions (lower plots). It can be observed that the broad-band resonator induces a shift of the nominal synchrotron frequency (all the satellites moving toward the central one). This shift is due to the term S_1 and the new nominal synchrotron frequency is $\Omega_0\sqrt{S_1}$. The broad-band resonator will reduce the nominal synchrotron frequency for

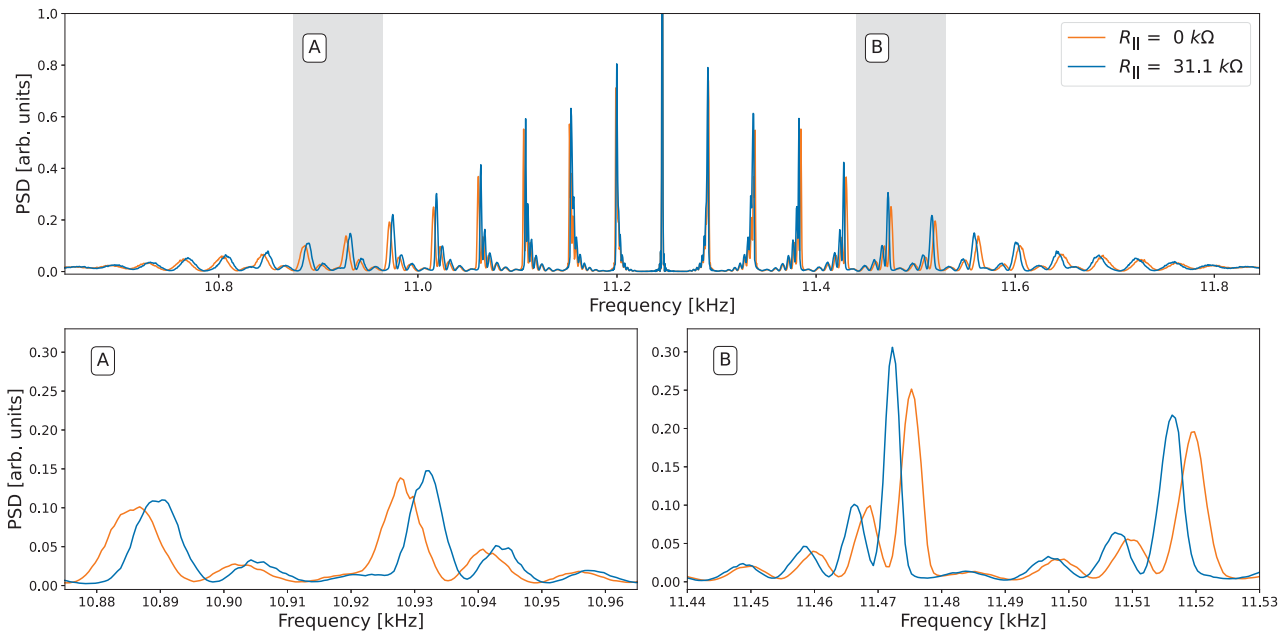

Figure 2: Simulated longitudinal Schottky spectra with (blue) and without (orange) an LHC-like broad-band resonator.

ISBN: 978-3-95450-236-3 ISSN: 2673-5350 doi:10.18429/JACoW-IBIC2023-WEP034

a machine operating above transition, as can be seen from Eq. (14) (the opposite happens below transition). One can also observe in Fig. 2 an amplitude-dependent synchrotron frequency shift, as the alterations in the satellite shapes can not be explained by a simple linear transformation involving shifting and scaling of the original form. This effect is due to the higher order terms $S_{2n+1},\ n \geq 1$ in Eq. (13).

Figure 3 compares the macro-particle simulation with the theoretical matrix formalism of Ref. [1], where the relation between synchrotron amplitudes and frequencies has been adapted, replacing Eq. (5) by Eq. (16) to take into account the effect of impedance. The dashed red line corresponds to the matrix formalism where only the first order term of the impedance contribution has been kept (i.e. $Z_1 \neq 0$ and $Z_3 = 0$, which corresponds to $S_1 = 1 - Z_1$ and $S_3 = -1/6$ in Eq. (16)). As can be seen, the nominal synchrotron frequency shift is well reproduced by the theory, while the shift for non-zero amplitude particles, requires higher order terms (Z_n).

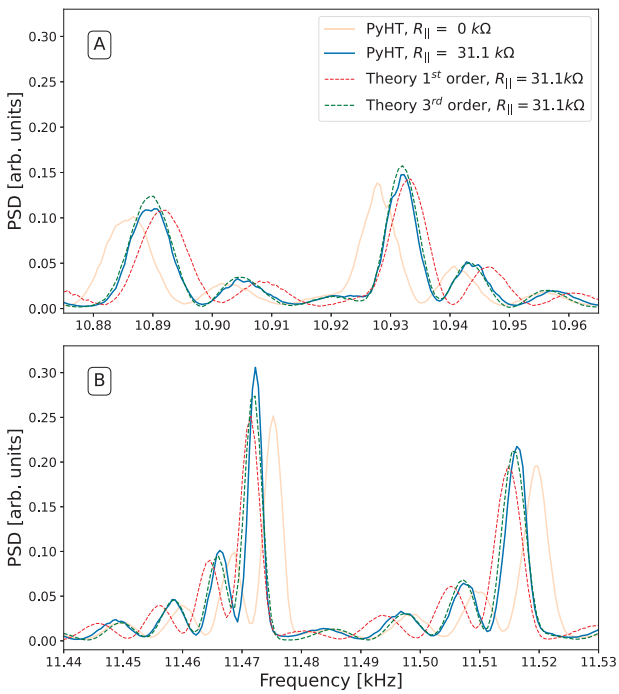

Figure 3: Comparison of the macro-particle simulation (blue) against the adapted matrix formalism, with Eq. (16) including impedance terms Z_n up to the first (red) and third (green) order. The A-B labels correspond to the shaded regions of Fig. 2.

The dashed green line also includes the third order term of the impedance contribution (i.e. $Z_1 \neq 0$ and $Z_3 \neq 0$, which corresponds to $S_1 = 1 - Z_1$ and $S_3 = -1/6 - Z_3$). With the third order impedance term, the theory is in good agreement with the simulation.

One can also probe the validity of Eq. (16) by directly extracting the relation $\Omega_s(\widehat{\phi})$ from the macro-particle simulation. This was done in Fig. 4 where each black dot corresponds to the synchrotron amplitude and frequency of a given macro-particle. As before, one can observe that the nominal synchrotron frequency shift is well reproduced by the first order term Z_1, while the shift for larger amplitude particles is correct with the third order theory, up to a certain amplitude $\widehat{\phi} \sim 1.25$ rad. In order to extend the region where Eq. (16) is valid, one would need to take into account the fifth order term S_5, in the equation of motion. However, this is not crucial since the majority of the particles are well described, as can be seen from the amplitude distribution.

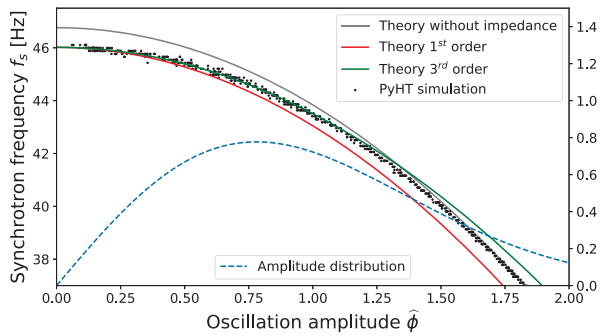

Figure 4: Comparison of Eq. (16) including impedance terms Z_n up to the first (red) and third (green) order, against macro-particle simulation (black dots).

CONCLUSION

The aim of this work was to explore the effects of longitudinal impedance on the Schottky spectrum. We first derived a longitudinal equation of motion including the forces coming from any impedance $Z(\omega)$. The particular case of a broad-band resonator was then studied in more detail and the relation between synchrotron amplitude and frequency was generalised to this situation, allowing existing theoretical reconstruction methods of Schottky spectra to include impedance effects. The developed theory was shown to be in good agreement with macro-particle simulations, by correctly reproducing the amplitude-dependent synchrotron tune shift.

REFERENCES

[1] K. Lasocha and D. Alves, "Estimation of longitudinal bunch characteristics in the LHC using Schottky-based diagnostics," *Phys. Rev. Accel. Beams*, vol. 23, no. 6, p. 062 803, 2020. doi:10.1103/PhysRevAccelBeams.23.062803

[2] K. Lasocha and D. Alves, "Estimation of transverse bunch characteristics in the lhc using schottky-based diagnostics," *Phys. Rev. Accel. Beams*, vol. 25, no. 6, p. 062 801, 2022. doi:10.1103/PhysRevAccelBeams.25.062801

ISBN: 978-3-95450-236-3 ISSN: 2673-5350 doi:10.18429/JACoW-IBIC2023-WEP034

[3] M. Betz, O. R. Jones, T. Lefevre, and M. Wendt, "Bunched-beam Schottky monitoring in the LHC," *Nucl. Instrum. Methods Phys. Res., A*, vol. 874, pp. 113–126, 2017. doi:10.1016/j.nima.2017.08.045

[4] C. Lannoy, D. Alves, N. Mounet, and T. Pieloni, "LHC Schottky Spectrum from Macro-Particle Simulations," in *Proc. IBIC'22*, Kraków, Poland, 2022, pp. 308–312. doi:10.18429/JACoW-IBIC2022-TUP34

[5] J. L. Laclare, "Bunched beam coherent instabilities," 1987. doi:10.5170/CERN-1987-003-V-1.264

[6] PyHEADTAIL code repository. https://github.com/PyCOMPLETE

[7] K. S. B. Li *et al.*, "Code Development for Collective Effects," in *Proc. HB'16*, Malmö, Sweden, Jul. 2016, pp. 362–367. doi:10.18429/JACoW-HB2016-WEAM3X01

[8] H. Wiedemann, *Particle accelerator physics*, 4th ed. Springer, 2015. doi:10.1007/978-3-319-18317-6

[9] Z. Szabó, "On the analytical methods approximating the time period of the nonlinear physical pendulum," *Periodica Polytechnica Mechanical Engineering*, vol. 48, no. 1, pp. 73–82, 2004. https://pp.bme.hu/me/article/view/1358

[10] I. Gradshteyn and I. Ryzhik, *Table of Integrals, Series, and Products*. 2007. http://fisica.ciens.ucv.ve/~svincenz/TISPISGIMR.pdf

[11] G. Stupakov, R. Lindberg, and B. Podobedov, "Wakefields and collective beam instabilities," in 2023. https://www.slac.stanford.edu/~stupakov/uspas23/2023-01-20/2022-12-07-LECTURES.pdf

[12] N. Mounet, "The LHC Transverse Coupled-Bunch Instability," Presented 2012, Ph.D. dissertation, 2012. doi:10.5075/epfl-thesis-5305